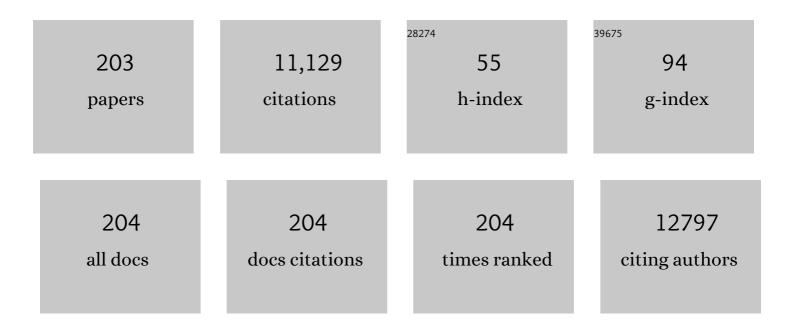
List of Publications by Year in descending order

Source: https://exaly.com/author-pdf/3378315/publications.pdf Version: 2024-02-01



**Shillinn Rao** 

#	Article	IF	CITATIONS
1	Carbon nanotube/polyaniline composite as anode material for microbial fuel cells. Journal of Power Sources, 2007, 170, 79-84.	7.8	564
2	New Nanostructured TiO <sub>2</sub> for Direct Electrochemistry and Glucose Sensor Applications. Advanced Functional Materials, 2008, 18, 591-599.	14.9	416
3	Nanostructured Polyaniline/Titanium Dioxide Composite Anode for Microbial Fuel Cells. ACS Nano, 2008, 2, 113-119.	14.6	381
4	Biomolecule-assisted synthesis of cobalt sulfide nanowires for application in supercapacitors. Journal of Power Sources, 2008, 180, 676-681.	7.8	315
5	Preparation of hexagonal nanoporous nickel hydroxide film and its application for electrochemical capacitor. Electrochemistry Communications, 2007, 9, 869-874.	4.7	279
6	Nanosized Metal Phosphides Embedded in Nitrogenâ€Đoped Porous Carbon Nanofibers for Enhanced Hydrogen Evolution at All pH Values. Angewandte Chemie - International Edition, 2018, 57, 1963-1967.	13.8	277
7	Honeycombâ€Like Spherical Cathode Host Constructed from Hollow Metallic and Polar Co <sub>9</sub> S <sub>8</sub> Tubules for Advanced Lithium–Sulfur Batteries. Advanced Functional Materials, 2018, 28, 1704443.	14.9	236
8	Doubleâ€5helled NiOâ€NiCo <sub>2</sub> O <sub>4</sub> Heterostructure@Carbon Hollow Nanocages as an Efficient Sulfur Host for Advanced Lithium–Sulfur Batteries. Advanced Energy Materials, 2018, 8, 1800709.	19.5	236
9	Well-Aligned Cone-Shaped Nanostructure of Polypyrrole/RuO <sub>2</sub> and Its Electrochemical Supercapacitor. Journal of Physical Chemistry C, 2008, 112, 14843-14847.	3.1	231
10	Electrocatalysis in microbial fuel cells—from electrode material to direct electrochemistry. Energy and Environmental Science, 2010, 3, 544.	30.8	225
11	Nanocubic KTi <sub>2</sub> (PO <sub>4</sub> ) <sub>3</sub> electrodes for potassium-ion batteries. Chemical Communications, 2016, 52, 11661-11664.	4.1	189
12	Mesoporous amorphous MnO2 as electrode material for supercapacitor. Journal of Solid State Electrochemistry, 2007, 11, 1101-1107.	2.5	187
13	Preparation and characterization of novel spinel Li4Ti5O12â^'xBrx anode materials. Electrochimica Acta, 2009, 54, 4772-4776.	5.2	175
14	Ni(II)-Based Metal-Organic Framework Anchored on Carbon Nanotubes for Highly Sensitive Non-Enzymatic Hydrogen Peroxide Sensing. Electrochimica Acta, 2016, 190, 365-370.	5.2	144
15	â€ <sup>-</sup> Circuit board-like CoS/MXene composite with superior performance for sodium storage. Chemical Engineering Journal, 2019, 357, 220-225.	12.7	143
16	Template-Free Electrochemical Synthesis of Superhydrophilic Polypyrrole Nanofiber Network. Macromolecules, 2008, 41, 7053-7057.	4.8	135
17	Shape Evolution and Magnetic Properties of Cobalt Sulfide. Crystal Growth and Design, 2008, 8, 3745-3749.	3.0	123
18	Bioinspired synthesis of nitrogen/sulfur co-doped graphene as an efficient electrocatalyst for oxygen reduction reaction. Journal of Power Sources, 2015, 279, 252-258.	7.8	117

#	Article	IF	CITATIONS
19	Novel porous anatase TiO2 nanorods and their high lithium electroactivity. Electrochemistry Communications, 2007, 9, 1233-1238.	4.7	112
20	Nitrogen-doped reduced-graphene oxide as an efficient metal-free electrocatalyst for oxygen reduction in fuel cells. RSC Advances, 2013, 3, 3990.	3.6	112
21	Self-assembly of three-dimensional interconnected graphene-based aerogels and its application in supercapacitors. Journal of Colloid and Interface Science, 2013, 407, 416-424.	9.4	111
22	Assembling Hollow Cobalt Sulfide Nanocages Array on Graphene-like Manganese Dioxide Nanosheets for Superior Electrochemical Capacitors. ACS Applied Materials & Interfaces, 2017, 9, 35040-35047.	8.0	107
23	Selenium Embedded in Metal–Organic Framework Derived Hollow Hierarchical Porous Carbon Spheres for Advanced Lithium–Selenium Batteries. ACS Applied Materials & Interfaces, 2016, 8, 16063-16070.	8.0	106
24	Design and Construction of Sodium Polysulfides Defense System for Roomâ€Temperature Na–S Battery. Advanced Science, 2019, 6, 1901557.	11.2	106
25	Metal chalcogenide hollow polar bipyramid prisms as efficient sulfur hosts for Na-S batteries. Nature Communications, 2020, 11, 5242.	12.8	102
26	Reunderstanding the Reaction Mechanism of Aqueous Zn–Mn Batteries with Sulfate Electrolytes: Role of the Zinc Sulfate Hydroxide. Advanced Materials, 2022, 34, e2109092.	21.0	97
27	Uniform α-Ni(OH)2 hollow spheres constructed from ultrathin nanosheets as efficient polysulfide mediator for long-term lithium-sulfur batteries. Energy Storage Materials, 2017, 8, 202-208.	18.0	93
28	Supercapacitance of Solid Carbon Nanofibers Made from Ethanol Flames. Journal of Physical Chemistry C, 2008, 112, 3612-3618.	3.1	83
29	Analysis of cobalt phosphide (CoP) nanorods designed for non-enzyme glucose detection. Analyst, The, 2016, 141, 256-260.	3.5	83
30	Synthesis and Electrical Transport of Novel Channel-StructuredÎ <sup>2</sup> -AgVO3. Small, 2007, 3, 1174-1177.	10.0	82
31	Self-assembled hierarchical graphene/polyaniline hybrid aerogels for electrochemical capacitive energy storage. Electrochimica Acta, 2014, 137, 381-387.	5.2	82
32	Tuning and thermal exfoliation graphene-like carbon nitride nanosheets for superior photocatalytic activity. Ceramics International, 2016, 42, 18521-18528.	4.8	82
33	Enhanced photocatalytic activity of magnetic TiO2 photocatalyst by silver deposition. Materials Letters, 2005, 59, 2194-2198.	2.6	75
34	Self-Supported FeCo <sub>2</sub> S <sub>4</sub> Nanotube Arrays as Binder-Free Cathodes for Lithium–Sulfur Batteries. ACS Applied Materials & Interfaces, 2018, 10, 43707-43715.	8.0	75
35	MXene-derivative pompon-like Na2Ti3O7@C anode material for advanced sodium ion batteries. Chemical Engineering Journal, 2019, 378, 122209.	12.7	75
36	Synthesis and electrochemical characterization of amorphous MnO2 for electrochemical capacitor. Materials Science & Engineering A: Structural Materials: Properties, Microstructure and Processing, 2005, 397, 305-309.	5.6	74

#	Article	IF	CITATIONS
37	Na <sub>3.12</sub> Fe <sub>2.44</sub> (P <sub>2</sub> O <sub>7</sub> ) <sub>2</sub> /multi-walled carbon nanotube composite as a cathode material for sodium-ion batteries. Journal of Materials Chemistry A, 2015, 3, 17224-17229.	10.3	74
38	Mesoporous Hollow Nitrogen-Doped Carbon Nanospheres with Embedded MnFe <sub>2</sub> O <sub>4</sub> /Fe Hybrid Nanoparticles as Efficient Bifunctional Oxygen Electrocatalysts in Alkaline Media. ACS Applied Materials & Interfaces, 2018, 10, 20440-20447.	8.0	73
39	NiMoO4 nanofibres designed by electrospining technique for glucose electrocatalytic oxidation. Analytica Chimica Acta, 2016, 905, 72-78.	5.4	72
40	Chinese knot-like electrode design for advanced Li-S batteries. Nano Energy, 2018, 53, 354-361.	16.0	72
41	Nanocrystalline nickel cobalt hydroxides/ultrastable Y zeolite composite for electrochemical capacitors. Journal of Solid State Electrochemistry, 2007, 11, 571-576.	2.5	71
42	Synthesis of M (Fe3C, Co, Ni)-porous carbon frameworks as high-efficient ORR catalysts. Energy Storage Materials, 2018, 11, 112-117.	18.0	71
43	A Fe3N/carbon composite electrocatalyst for effective polysulfides regulation in room-temperature Na-S batteries. Nature Communications, 2021, 12, 6347.	12.8	71
44	Highly ordered MnO2 nanowire array thin films on Ti/Si substrate as an electrode for electrochemical capacitor. Journal of Solid State Chemistry, 2006, 179, 1351-1355.	2.9	70
45	Nickel Hollow Spheres Concatenated by Nitrogenâ€Doped Carbon Fibers for Enhancing Electrochemical Kinetics of Sodium–Sulfur Batteries. Advanced Science, 2020, 7, 1902617.	11.2	70
46	Novel mesoporous MnO2 for high-rate electrochemical capacitive energy storage. Electrochimica Acta, 2010, 55, 5117-5122.	5.2	68
47	TiOxNy nanoparticles/C composites derived from MXene as anode material for potassium-ion batteries. Chemical Engineering Journal, 2019, 369, 828-833.	12.7	68
48	Amorphous nickel sulfide nanosheets with embedded vanadium oxide nanocrystals on nickel foam for efficient electrochemical water oxidation. Journal of Materials Chemistry A, 2019, 7, 10534-10542.	10.3	65
49	Lowâ€Operating Temperature, Highâ€Rate and Durable Solidâ€State Sodiumâ€Ion Battery Based on Polymer Electrolyte and Prussian Blue Cathode. Advanced Energy Materials, 2020, 10, 1903351.	19.5	64
50	Carbon nanotubes implanted manganese-based MOFs for simultaneous detection of biomolecules in body fluids. Analyst, The, 2016, 141, 1279-1285.	3.5	62
51	A railway-like network electrode design for room temperature Na–S battery. Journal of Materials Chemistry A, 2019, 7, 150-156.	10.3	60
52	Multimodal porous CNT@TiO2 nanocables with superior performance in lithium-ion batteries. Journal of Materials Chemistry A, 2013, 1, 8525.	10.3	59
53	Nanostructured cobalt phosphates as excellent biomimetic enzymes to sensitively detect superoxide anions released from living cells. Biosensors and Bioelectronics, 2017, 87, 998-1004.	10.1	59
54	MoP nanoparticles with a P-rich outermost atomic layer embedded in N-doped porous carbon nanofibers: Self-supported electrodes for efficient hydrogen generation. Nano Research, 2018, 11, 4728-4734.	10.4	59

#	Article	IF	CITATIONS
55	Preparation of MoS <sub>2</sub> /Ti <sub>3</sub> C <sub>2</sub> T <sub>x</sub> composite as anode material with enhanced sodium/lithium storage performance. Inorganic Chemistry Frontiers, 2019, 6, 117-125.	6.0	59
56	Rational construction of rGO/VO2 nanoflowers as sulfur multifunctional hosts for room temperature Na-S batteries. Chemical Engineering Journal, 2020, 379, 122359.	12.7	59
57	Interface engineered construction of porous g-C3N4/TiO2 heterostructure for enhanced photocatalysis of organic pollutants. Applied Surface Science, 2018, 440, 229-236.	6.1	58
58	Nanosized Metal Phosphides Embedded in Nitrogenâ€Đoped Porous Carbon Nanofibers for Enhanced Hydrogen Evolution at All pH Values. Angewandte Chemie, 2018, 130, 1981-1985.	2.0	58
59	Synthesis and application of ultra-long Na <sub>0.44</sub> MnO <sub>2</sub> submicron slabs as a cathode material for Na-ion batteries. RSC Advances, 2014, 4, 38140-38143.	3.6	57
60	Confined selenium within metal-organic frameworks derived porous carbon microcubes as cathode for rechargeable lithium–selenium batteries. Journal of Power Sources, 2017, 341, 53-59.	7.8	56
61	Investigation of Fe <sub>2</sub> N@carbon encapsulated in N-doped graphene-like carbon as a catalyst in sustainable zinc–air batteries. Catalysis Science and Technology, 2017, 7, 5670-5676.	4.1	56
62	Efficient in situ growth of enzyme-inorganic hybrids on paper strips for the visual detection of glucose. Biosensors and Bioelectronics, 2018, 99, 603-611.	10.1	56
63	Engineering the nanostructure of molybdenum nitride nanodot embedded N-doped porous hollow carbon nanochains for rapid all pH hydrogen evolution. Journal of Materials Chemistry A, 2018, 6, 14734-14741.	10.3	56
64	Morphology and electrochemistry of LiMn2O4 optimized by using different Mn-sources. Journal of Power Sources, 2007, 164, 885-889.	7.8	54
65	Porous graphene to encapsulate Na <sub>6.24</sub> Fe <sub>4.88</sub> (P <sub>2</sub> O <sub>7</sub> ) <sub>4</sub> as composite cathode materials for Na-ion batteries. Chemical Communications, 2015, 51, 13120-13122.	4.1	51
66	Analysis of graphene-like activated carbon derived from rice straw for application in supercapacitor. Chinese Chemical Letters, 2017, 28, 2290-2294.	9.0	51
67	MXene-derived three-dimensional carbon nanotube network encapsulate CoS <sub>2</sub> nanoparticles as an anode material for solid-state sodium-ion batteries. Journal of Materials Chemistry A, 2020, 8, 3018-3026.	10.3	51
68	A gel-limiting strategy for large-scale fabrication of Fe–N–C single-atom ORR catalysts. Journal of Materials Chemistry A, 2021, 9, 7137-7142.	10.3	51
69	Synthesis and electrochemical properties of LiAl0.1Mn1.9O4 by microwave-assisted sol–gel method. Journal of Power Sources, 2006, 154, 239-245.	7.8	49
70	Yolk-shell porous carbon spheres@CoSe2 nanosheets as multilayer defenses system of polysulfide for advanced Li-S batteries. Chemical Engineering Journal, 2021, 413, 127521.	12.7	49
71	Facile synthesis of Ag/ZnO nanorods using Ag/C cables as templates and their gas-sensing properties. Materials Letters, 2010, 64, 243-245.	2.6	48
72	Puzzle-inspired carbon dots coupled with cobalt phosphide for constructing a highly-effective overall water splitting interface. Chemical Communications, 2020, 56, 257-260.	4.1	48

#	Article	IF	CITATIONS
73	A rough endoplasmic reticulum-like VSe <sub>2</sub> /rGO anode for superior sodium-ion capacitors. Inorganic Chemistry Frontiers, 2019, 6, 2935-2943.	6.0	46
74	Environment-friendly biomimetic synthesis of TiO <sub>2</sub> nanomaterials for photocatalytic application. Nanotechnology, 2012, 23, 205601.	2.6	44
75	A facile route for constructing a graphene-chitosan-ZrO2 composite for direct electron transfer and glucose sensing. RSC Advances, 2012, 2, 8172.	3.6	44
76	Design and synthesis of Co–N–C porous catalyst derived from metal organic complexes for highly effective ORR. Dalton Transactions, 2017, 46, 15646-15650.	3.3	44
77	Ultrafine TiO2 encapsulated in nitrogen-doped porous carbon framework for photocatalytic degradation of ammonia gas. Chemical Engineering Journal, 2018, 331, 383-388.	12.7	44
78	Potassium titanium hexacyanoferrate as a cathode material for potassium-ion batteries. Journal of Physics and Chemistry of Solids, 2018, 122, 31-35.	4.0	43
79	Synthesis of Cobalt Phosphide Nanoparticles Supported on Pristine Graphene by Dynamically Selfâ€Assembled Graphene Quantum Dots for Hydrogen Evolution. ChemSusChem, 2017, 10, 1014-1021.	6.8	42
80	Self-Supported CdP <sub>2</sub> –CDs–CoP for High-Performance OER Catalysts. ACS Sustainable Chemistry and Engineering, 2021, 9, 1297-1303.	6.7	42
81	Significantly fastened redox kinetics in single crystal layered oxide cathode by gradient doping. Nano Energy, 2022, 94, 106961.	16.0	42
82	Interfacial engineering of Ni/V2O3 for hydrogen evolution reaction. Nano Research, 2020, 13, 2407-2412.	10.4	41
83	Synthesis and electrochemical properties of LiAl0.05Mn1.95O4 by the ultrasonic assisted rheological phase method. Electrochimica Acta, 2006, 51, 4701-4708.	5.2	40
84	Muscle-like electrode design for Li-Te batteries. Energy Storage Materials, 2018, 10, 10-15.	18.0	40
85	Double-walled N-doped carbon@NiCo <sub>2</sub> S <sub>4</sub> hollow capsules as SeS <sub>2</sub> hosts for advanced Li–SeS <sub>2</sub> batteries. Journal of Materials Chemistry A, 2019, 7, 12276-12282.	10.3	40
86	Nanoporous V-Doped Ni <sub>5</sub> P <sub>4</sub> Microsphere: A Highly Efficient Electrocatalyst for Hydrogen Evolution Reaction at All pH. ACS Applied Materials & Interfaces, 2020, 12, 37092-37099.	8.0	40
87	A synergistic Bi <sub>2</sub> S <sub>3</sub> /MXene composite with enhanced performance as an anode material of sodium-ion batteries. New Journal of Chemistry, 2020, 44, 3072-3077.	2.8	40
88	A 3D porous interconnected NaVPO <sub>4</sub> F/C network: preparation and performance for Na-ion batteries. RSC Advances, 2015, 5, 40065-40069.	3.6	39
89	Efficient Catalytic Conversion of Polysulfides by Biomimetic Design of "Branch-Leaf―Electrode for High-Energy Sodium–Sulfur Batteries. Nano-Micro Letters, 2021, 13, 50.	27.0	39
90	Lithium Insertion in Channel-Structured β-AgVO <sub>3</sub> : <i>In Situ</i> Raman Study and Computer Simulation. Chemistry of Materials, 2007, 19, 5965-5972.	6.7	37

#	Article	IF	CITATIONS
91	Synthesis and photoluminescence of Eu2+ by co-doping Eu3+ and Clâ^' in Sr2P2O7 under air atmosphere. Journal of Alloys and Compounds, 2012, 512, 323-327.	5.5	37
92	Improving the Performance of Hard Carbon//Na <sub>3</sub> V <sub>2</sub> O <sub>2</sub> (PO <sub>4</sub> ) <sub>2</sub> F Sodium-Ion Full Cells by Utilizing the Adsorption Process of Hard Carbon. ACS Applied Materials & Interfaces, 2018, 10, 16581-16587.	8.0	37
93	Vanadium carbide nanoparticles incorporation in carbon nanofibers for room-temperature sodium sulfur batteries: Confining, trapping, and catalyzing. Chemical Engineering Journal, 2020, 395, 124978.	12.7	37
94	A highly-effective nitrogen-doped porous carbon sponge electrode for advanced K–Se batteries. Inorganic Chemistry Frontiers, 2020, 7, 1182-1189.	6.0	36
95	Novel Oxygen-Deficient Zirconia (ZrO <sub>2–<i>x</i></sub> ) for Fluorescence/Photoacoustic Imaging-Guided Photothermal/Photodynamic Therapy for Cancer. ACS Applied Materials & Interfaces, 2019, 11, 41127-41139.	8.0	35
96	Effective microwave-assisted synthesis of graphenenanosheets/NiO composite for high-performance supercapacitors. New Journal of Chemistry, 2013, 37, 439-443.	2.8	34
97	Cobalt nanoparticles embedded into free-standing carbon nanofibers as catalyst for room-temperature sodium-sulfur batteries. Journal of Colloid and Interface Science, 2020, 565, 63-69.	9.4	34
98	Significance of gallium doping for high Ni, low Co/Mn layered oxide cathode material. Chemical Engineering Journal, 2022, 441, 135821.	12.7	34
99	An excellent full sodium-ion capacitor derived from a single Ti-based metal–organic framework. Journal of Materials Chemistry A, 2018, 6, 24860-24868.	10.3	33
100	Bismuth oxychloride ultrathin nanoplates as an anode material for sodium-ion batteries. Materials Letters, 2016, 178, 44-47.	2.6	32
101	Jackfruit-like electrode design for advanced Na-Se batteries. Journal of Power Sources, 2019, 443, 227245.	7.8	32
102	A Strategy for Polysulfides/Polyselenides Protection Based on Co <sub>9</sub> S <sub>8</sub> @SiO <sub>2</sub> /C Host in Na‣eS <sub>2</sub> Batteries. Advanced Functional Materials, 2021, 31, 2001952.	14.9	32
103	An architectural development for energy conversion materials: morphology-conserved transformation synthesis of manganese oxides and their application in lithium ion batteries. Journal of Materials Chemistry A, 2014, 2, 3749.	10.3	31
104	(001) Facet-Dominated Hierarchically Hollow Na <sub>2</sub> Ti <sub>3</sub> O <sub>7</sub> as a High-Rate Anode Material for Sodium-Ion Capacitors. ACS Applied Materials & Interfaces, 2019, 11, 42197-42205.	8.0	31
105	High-Rate and Long-Life Sodium-Ion Batteries Based on Sponge-like Three-Dimensional Porous Na-Rich Ferric Pyrophosphate Cathode Material. ACS Applied Materials & Interfaces, 2019, 11, 5107-5113.	8.0	30
106	Synthesis and electrochemical properties of LiMn2O4 by microwave-assisted sol–gel method. Materials Letters, 2005, 59, 3761-3765.	2.6	29
107	Flower-like NiO structures: Controlled hydrothermal synthesis and electrochemical characteristic. Materials Research Bulletin, 2012, 47, 3947-3951.	5.2	29
108	Exploration of a calcium–organic framework as an anode material for sodium-ion batteries. Chemical Communications, 2016, 52, 9969-9971.	4.1	29

#	Article	IF	CITATIONS
109	Constructing high effective nano-Mn3(PO4)2-chitosan in situ electrochemical detection interface for superoxide anions released from living cell. Biosensors and Bioelectronics, 2019, 133, 133-140.	10.1	29
110	A self-healing neutral aqueous rechargeable Zn/MnO2 battery based on modified carbon nanotubes substrate cathode. Journal of Colloid and Interface Science, 2021, 600, 83-89.	9.4	29
111	Ni/Li antisite induced disordered passivation layer for high-Ni layered oxide cathode material. Energy Storage Materials, 2022, 45, 720-729.	18.0	29
112	Synthesis and electrochemical properties of chemically substituted LiMn2O4 prepared by a solution-based gel method. Journal of Colloid and Interface Science, 2006, 300, 633-639.	9.4	28
113	Plastic protein microarray to investigate the molecular pathways of magnetic nanoparticle-induced nanotoxicity. Nanotechnology, 2013, 24, 175501.	2.6	28
114	MnO <sub>2</sub> -assisted fabrication of PANI/MWCNT composite and its application as a supercapacitor. RSC Advances, 2014, 4, 33569-33573.	3.6	28
115	Cobalt nanoparticle decorated graphene aerogel for efficient oxygen reduction reaction electrocatalysis. International Journal of Hydrogen Energy, 2017, 42, 5930-5937.	7.1	28
116	Three-dimensional hierarchical porous tubular carbon as a host matrix for long-term lithium-selenium batteries. Journal of Power Sources, 2017, 367, 17-23.	7.8	28
117	Metal-organic complex derived hierarchical porous carbon as host matrix for rechargeable Na-Se batteries. Electrochimica Acta, 2018, 276, 21-27.	5.2	28
118	Hydrothermal synthesis of single-crystal VO2(B) nanobelts. Materials Research Bulletin, 2006, 41, 1985-1989.	5.2	27
119	Effect of alkaline and alkaline–earth cations on the supercapacitor performance of MnO2 with various crystallographic structures. Journal of Solid State Electrochemistry, 2013, 17, 1357-1368.	2.5	27
120	FePO4 embedded in nanofibers consisting of amorphous carbon and reduced graphene oxide asÂan enzyme mimetic for monitoring superoxide anions released by living cells. Mikrochimica Acta, 2018, 185, 140.	5.0	27
121	Lowâ€Barrier, Dendriteâ€Free, and Stable Na Plating/Stripping Enabled by Gradient Sodiophilic Carbon Skeleton. Advanced Energy Materials, 2021, 11, .	19.5	27
122	One-Step, Low-Temperature Route for the Preparation of Spinel LiMn[sub 2]O[sub 4] as a Cathode Material for Rechargeable Lithium Batteries. Journal of the Electrochemical Society, 2005, 152, A2030.	2.9	26
123	Micropore-Boosted Layered Double Hydroxide Catalysts: EIS Analysis in Structure and Activity for Effective Oxygen Evolution Reactions. ACS Applied Materials & Interfaces, 2019, 11, 30887-30893.	8.0	26
124	Flexible electrode constructed by encapsulating ultrafine VSe2 in carbon fiber for quasi-solid-state sodium ion batteries. Journal of Power Sources, 2020, 470, 228438.	7.8	25
125	Identification of Catalytic Active Sites for Durable Proton Exchange Membrane Fuel Cell: Catalytic Degradation and Poisoning Perspectives. Small, 2022, 18, e2106279.	10.0	25
126	Design and synthesis of carbonized polypyrrole-coated graphene aerogel acting as an efficient metal-free catalyst for oxygen reduction. RSC Advances, 2014, 4, 16979-16984.	3.6	24

#	Article	IF	CITATIONS
127	A selenium-confined porous carbon cathode from silk cocoons for Li–Se battery applications. RSC Advances, 2015, 5, 96146-96150.	3.6	24
128	Facile and Scale Synthesis of Co/N/S-Doped Porous Graphene-Like Carbon Architectures as Electrocatalysts for Sustainable Zinc-Air Battery Cells. ACS Sustainable Chemistry and Engineering, 2019, 7, 7743-7749.	6.7	24
129	Multi-step Controllable Catalysis Method for the Defense of Sodium Polysulfide Dissolution in Room-Temperature Na–S Batteries. ACS Applied Materials & Interfaces, 2021, 13, 11852-11860.	8.0	24
130	A new calcium metal organic frameworks (Ca-MOF) for sodium ion batteries. Materials Letters, 2021, 286, 129264.	2.6	24
131	A green and facile route for constructing flower-shaped TiO <sub>2</sub> nanocrystals assembled on graphene oxide sheets for enhanced photocatalytic activity. Nanotechnology, 2013, 24, 275602.	2.6	23
132	Biomass-derived synthesis of nitrogen and phosphorus Co-doped mesoporous carbon spheres as catalysts for oxygen reduction reaction. Journal of Solid State Electrochemistry, 2017, 21, 103-110.	2.5	23
133	Enhancement of the electrochemical properties of LiMn2O4 through Al3+ and Fâ^' co-substitution. Journal of Colloid and Interface Science, 2005, 291, 433-437.	9.4	22
134	Environmentally-friendly biomimicking synthesis of TiO2 nanomaterials using saccharides to tailor morphology, crystal phase and photocatalytic activity. CrystEngComm, 2013, 15, 4694.	2.6	22
135	Bimetal–organic-frameworks-derived yolk–shell-structured porous Co <sub>2</sub> P/ZnO@PC/CNTs hybrids for highly sensitive non-enzymatic detection of superoxide anion released from living cells. Chemical Communications, 2016, 52, 12442-12445.	4.1	22
136	Aspergillus flavus Conidia-derived Carbon/Sulfur Composite as a Cathode Material for High Performance Lithium–Sulfur Battery. Scientific Reports, 2016, 6, 18739.	3.3	22
137	Controlled synthesis of Mn3(PO4)2 hollow spheres as biomimetic enzymes for selective detection of superoxide anions released by living cells. Mikrochimica Acta, 2017, 184, 1177-1184.	5.0	22
138	Porous carbon derived from Sunflower as a host matrix for ultra-stable lithium–selenium battery. Journal of Colloid and Interface Science, 2017, 490, 747-753.	9.4	22
139	Highly efficient Fe-N-C oxygen reduction electrocatalyst engineered by sintering atmosphere. Journal of Power Sources, 2020, 449, 227497.	7.8	22
140	Novel CdFe Bimetallic Complex-Derived Ultrasmall Fe- and N-Codoped Carbon as a Highly Efficient Oxygen Reduction Catalyst. ACS Applied Materials & Interfaces, 2019, 11, 21481-21488.	8.0	21
141	Synthesis and electrochemical properties of nanostructured LiAl x Mn2 â^ x O4 â^ y Br y part of Solid State Electrochemistry, 2009, 13, 799-805.	cles. Jourr 2.5	nal <sub>20</sub>
142	Self-assembled three-dimensional interpenetrating porous graphene aerogels with MnO2 coating and their application as high-performance supercapacitors. New Journal of Chemistry, 2013, 37, 4199.	2.8	20
143	Low-operating temperature quasi-solid-state potassium-ion battery based on commercial materials. Journal of Colloid and Interface Science, 2021, 582, 932-939.	9.4	20
144	Preparation and electrochemical properties of LiMn2O4 by the microwave-assisted rheological phase method. Electrochimica Acta, 2007, 52, 3286-3293.	5.2	19

#	Article	IF	CITATIONS
145	One step microwave synthesis and magnetic properties of Co3O4 octahedrons. Materials Letters, 2012, 83, 195-197.	2.6	19
146	Template method for fabricating Co and Ni nanoparticles/porous channels carbon for solid-state sodium-sulfur battery. Journal of Colloid and Interface Science, 2020, 578, 710-716.	9.4	19
147	MIL-47(V) catalytic conversion of H2O2 for sensitive H2O2 detection and tumor cell inhibition. Sensors and Actuators B: Chemical, 2022, 354, 131201.	7.8	19
148	Electrochemical properties and synthesis of LiAl0.05Mn1.95O3.95F0.05 by a solution-based gel method for lithium secondary battery. Journal of Solid State Chemistry, 2005, 178, 897-901.	2.9	18
149	Enhancement of the electrochemical properties of LiMn2O4 through chemical substitution. Materials Chemistry and Physics, 2006, 95, 188-192.	4.0	18
150	LiMn2O4–yBr y Nanoparticles Synthesized by a Room Temperature Solid-State Coordination Method. Nanoscale Research Letters, 2009, 4, 353-358.	5.7	18
151	Synthesis and electrochemical properties of nanosized carbon-coated Li1â^'3x La x FePO4 composites. Journal of Solid State Electrochemistry, 2010, 14, 889-895.	2.5	18
152	Rapid synthesis of Mn3O4 by in-situ redox method and its capacitive performances. Rare Metals, 2011, 30, 81-84.	7.1	18
153	pH-controllable synthesis of unique nanostructured tungsten oxide aerogel and its sensitive glucose biosensor. Nanotechnology, 2015, 26, 115602.	2.6	18
154	Three-dimensional nanotubes composed of carbon-anchored ultrathin MoS <sub>2</sub> nanosheets with enhanced lithium storage. Physical Chemistry Chemical Physics, 2016, 18, 19792-19797.	2.8	18
155	Ternary Ni <sub><i>x</i></sub> Co <sub>3â^'<i>x</i></sub> S <sub>4</sub> with a Fine Hollow Nanostructure as a Robust Electrocatalyst for Hydrogen Evolution. ChemCatChem, 2017, 9, 4169-4174.	3.7	18
156	Nitrogenâ€Doped Carbon as a Host for Tellurium for Highâ€Rate Li–Te and Na–Te Batteries. ChemSusChem, 2019, 12, 1196-1202.	6.8	18
157	BC@DNA-Mn <sub>3</sub> (PO <sub>4</sub> ) <sub>2</sub> Nanozyme for Real-Time Detection of Superoxide from Living Cells. Analytical Chemistry, 2020, 92, 15927-15935.	6.5	18
158	In situ synthesis and excellent photocatalytic activity of tiny Bi decorated bismuth tungstate nanorods. RSC Advances, 2015, 5, 85500-85505.	3.6	17
159	Hierarchical growth of vertically standing Fe3O4-FeSe/CoSe2 nano-array for high effective oxygen evolution reaction. Materials Research Bulletin, 2020, 122, 110680.	5.2	17
160	Electrospinning Synthesis of Porous CoWO <sub>4</sub> Nanofibers as an Ultrasensitive, Nonenzymatic, Hydrogenâ€Peroxide‧ensing Interface with Enhanced Electrocatalysis. ChemElectroChem, 2015, 2, 2061-2070.	3.4	15
161	An iron hydroxyl phosphate microoctahedron catalyst as an efficient peroxidase mimic for sensitive and colorimetric quantification of H <sub>2</sub> O <sub>2</sub> and glucose. New Journal of Chemistry, 2018, 42, 6803-6809.	2.8	15
162	A labyrinth-like network electrode design for lithium–sulfur batteries. Nanoscale, 2019, 11, 14648-14653.	5.6	15

#	Article	IF	CITATIONS
163	Ultrafast kinetics and high capacity for Stable Sodium Storage enabled by Fe3Se4/ZnSe heterostructure engineering. Composites Part B: Engineering, 2021, 224, 109166.	12.0	15
164	Flexible MXene-Ti3C2Tx bond few-layers transition metal dichalcogenides MoS2/C spheres for fast and stable sodium storage. Chemical Engineering Journal, 2022, 427, 130960.	12.7	15
165	Propelling the practical application of the intimate coupling of photocatalysis and biodegradation system: System amelioration, environmental influences and analytical strategies. Chemosphere, 2022, 287, 132196.	8.2	15
166	Chessboard structured electrode design for Li-S batteries Based on MXene nanosheets. Chemical Engineering Journal, 2022, 429, 131997.	12.7	15
167	Effects of Reaction Temperature on Microstructure and Advanced Pseudocapacitor Properties of NiO Prepared via Simple Precipitation Method. Nano-Micro Letters, 2013, 5, 289-295.	27.0	14
168	Design and fabrication of highly sensitive and stable biochip for glucose biosensing. Applied Surface Science, 2017, 422, 900-904.	6.1	14
169	Design, synthesis and photodegradation ammonia properties of MoS2@TiO2 encapsulated carbon coaxial nanobelts. Materials Letters, 2017, 209, 56-59.	2.6	14
170	Suppressed shuttling effect of polysulfides using three-dimensional nickel hydroxide polyhedrons for advanced lithium-sulfur batteries. Journal of Colloid and Interface Science, 2021, 593, 89-95.	9.4	14
171	Heterogeneous interface designing of bimetallic selenides nanocubes for superior sodium storage. Journal of Power Sources, 2021, 506, 230249.	7.8	14
172	A facile and well-tailored vanadium oxide porous network for high-capacity electrochemical capacitive energy storage. Materials Letters, 2014, 120, 283-286.	2.6	13
173	Platanus hispanica-inspired design of Co–carbon nanotube frameworks through chemical vapor deposition: a highly integrated hierarchical electrocatalyst for oxygen reduction reactions. Chemical Communications, 2016, 52, 12992-12995.	4.1	13
174	Photocatalytic activity of Pt-modified Bi2WO6 nanoporous wall under sunlight. Journal of Nanoparticle Research, 2015, 17, 1.	1.9	12
175	The construction of ZnS–In <sub>2</sub> S <sub>3</sub> nanonests and their heterojunction boosted visible-light photocatalytic/photoelectrocatalytic performance. New Journal of Chemistry, 2019, 43, 14402-14408.	2.8	12
176	Experimental investigation of the important influence of pretreatment process of thermally exfoliated graphene on their microstructure and supercapacitor performance. Electrochimica Acta, 2015, 180, 187-195.	5.2	11
177	CdMn Bimetallic Complex-Derived Manganese–Nitrogen Species as Electrocatalysts for an Oxygen Reduction Reaction. ACS Sustainable Chemistry and Engineering, 2020, 8, 12618-12625.	6.7	11
178	Na 3 V 2 O 2 (PO 4 ) 2 F Cathode for Highâ€Performance Quasiâ€Solidâ€State Sodiumâ€Ion Batteries with a Wic Workable Temperature Range. Energy Technology, 2020, 8, 2000494.	<sup>le</sup> 3.8	11
179	Synthesis of sodium manganese oxides with tailored multi-morphologies and their application in lithium/sodium ion batteries. RSC Advances, 2014, 4, 30340.	3.6	10
180	Design of an amperometric glucose oxidase biosensor with added protective and adhesion layers. Mikrochimica Acta, 2021, 188, 312.	5.0	10

#	Article	IF	CITATIONS
181	A series of spinel phase cathode materials prepared by a simple hydrothermal process for rechargeable lithium batteries. Journal of Solid State Chemistry, 2006, 179, 2133-2140.	2.9	9
182	In situ growth of metallic silver on glucose oxidase for a highly sensitive glucose sensor. RSC Advances, 2015, 5, 34486-34490.	3.6	9
183	Evaluation of O3-type Na0.8Ni0.6Sb0.4O2 as cathode materials for sodium-ion batteries. Journal of Solid State Electrochemistry, 2016, 20, 2331-2335.	2.5	9
184	Nanostring-cluster hierarchical structured Bi <sub>2</sub> O <sub>3</sub> : synthesis, evolution and application in biosensing. Physical Chemistry Chemical Physics, 2016, 18, 1931-1936.	2.8	9
185	Why does the capacity of vanadium selenide based aqueous zinc ion batteries continue to increase during long cycles?. Journal of Colloid and Interface Science, 2022, 615, 30-37.	9.4	9
186	Influence of cation (NH4+) on electrochemical characteristics of MnO2 nanowire synthesized by hydrothermal method. Journal of Solid State Electrochemistry, 2005, 9, 655-659.	2.5	8
187	Synthesis and electrochemical properties of spinel LiMn2O4 prepared by the rheological phase method. Journal of Solid State Electrochemistry, 2006, 10, 277-282.	2.5	8
188	Self-assembled three-dimensional graphene/OMCs hybrid aerogels for high-rate supercapacitive energy storage. RSC Advances, 2013, 3, 25317.	3.6	8
189	In situ synthesis and analytical investigation of porous Hb–Mn3(PO4)2 hybrid nanosheets and their biosensor applications. RSC Advances, 2016, 6, 95199-95203.	3.6	8
190	A new polyanionic cathode with stable structure and superior kinetics for Na-ion batteries. Chemical Engineering Journal, 2021, 405, 127035.	12.7	8
191	Gelation of organic liquid electrolyte to achieve superior sodium-ion full-cells. Journal of Colloid and Interface Science, 2021, 599, 190-197.	9.4	8
192	Anthozoan-like porous nanocages with nano-cobalt-armed CNT multifunctional layers as a cathode material for highly stable Na–S batteries. Inorganic Chemistry Frontiers, 2022, 9, 645-651.	6.0	7
193	A distinctive conversion mechanism for reversible zinc ion storage. Inorganic Chemistry Frontiers, 2022, 9, 2706-2713.	6.0	7
194	3D interpenetrating macroporous graphene aerogels with MnO2 coating for supercapacitors. Russian Journal of Electrochemistry, 2015, 51, 782-788.	0.9	6
195	Ascorbic acid-tailored synthesis of carbon-wrapped nanocobalt encapsulated in graphene aerogel as electrocatalysts for highly effective oxygen-reduction reaction. Journal of Solid State Electrochemistry, 2017, 21, 3641-3648.	2.5	6
196	Hollow Co <sub>3</sub> O <sub>4</sub> Nanocages Decorated Graphene Aerogels Derived from Carbon Wrapped Nanoâ€Co for Efficient Oxygen Reduction Reaction. ChemistrySelect, 2017, 2, 6359-6363.	1.5	6
197	Tessellated N-doped carbon/CoSe <sub>2</sub> as trap-catalyst sulfur hosts for room-temperature sodium–sulfur batteries. Inorganic Chemistry Frontiers, 2022, 9, 1743-1751.	6.0	6
198	Carbon dots-induced carbon-coated Ni and Mo2N nanosheets for efficient hydrogen production. Electrochimica Acta, 2022, 424, 140671.	5.2	6

#	Article	IF	CITATIONS
199	High-rate and non-toxic Na <sub>7</sub> Fe <sub>4.5</sub> (P <sub>2</sub> O <sub>7</sub> ) <sub>4</sub> @C for quasi-solid-state sodium-ion batteries. Materials Chemistry Frontiers, 2021, 5, 2783-2790.	5.9	3
200	A facilely-synthesized polyanionic cathode with impressive long-term cycling stability for sodium-ion batteries. Chemical Communications, 2021, 57, 9566-9569.	4.1	2
201	A coaxial nanocable textured by a cerium oxide shell and carbon core for sensing nitric oxide. Mikrochimica Acta, 2019, 186, 789.	5.0	1
202	Designing 2D nickel hydroxide@graphene nanosheet composites to confine sulfur in highly stable lithium–sulfur batteries. Sustainable Energy and Fuels, 2021, 5, 5175-5183.	4.9	1
203	Bacterial cellulose network based gel polymer electrolyte for quasi-solid-state sodium-ion battery. Journal of Materials Science: Materials in Electronics, 0, , .	2.2	1